Layout: T1 Standard | Book ID: 417756_1_En | Book ISBN: 978-981-10-1925-8
Chapter No.: 37 | Date: 12-8-2016 Time: 2:12 pm | Page: 1/9

Finite-Discrete Element Analysis of Interface Shear Damage to HDPE Geomembrane in Contact with Gravel Drainage Layer

Masood Meidani, Mohamed A. Meguid and Luc E. Chouinard

Abstract High density polyethylene (HDPE) geomembrane (GM) is usually used as a hydraulic barrier in waste containment applications including municipal solid waste facilities. Stress concentration resulting from direct contact with stones, gravel and other drainage material may cause significant damage to the GM sheet. Protection layers are generally used to keep the GM safe against puncture and tear. However, GM sheets are sometimes placed directly under crushed stones drainage layer containing relatively large size particles protruding from the surface. Under these conditions, interface shear displacement may develop within the liner system causing damage to the GM material. In this study a coupled finite-discrete framework has been developed to investigate the behaviour of a gravel drainage layer located above HDPE geomembrane sheet and subject to moderate to high normal stress conditions. The geomembrane is modelled using finite elements (FE) whereas the drainage layer and the underlying foundation are modelled using discrete elements (DE). Numerical simulation is performed based existing experimental results for the same configuration and detailed behaviour of the GM sheet is then investigated. Results show that shear displacement developing between the drainage layer and the HDPE geomembrane should be considered in the design of landfill barrier system.

1 Introduction

High-density polyethylene (HDPE) geomembrane (GM) is usually used as a hydraulic barrier in waste containment applications including municipal solid waste facilities. One of the greatest risks of damage to geomembrane arises from holes created during installation or stress concentration caused by contact with overlying coarse gravel particles over a period of time [8]. Soil-GM interface acts as a possible plane of instability under different load conditions. Interface shear

M. Meidani · M.A. Meguid (✉) · L.E. Chouinard
Civil Engineering and Applied Mechanics, McGill University, Montreal, Canada
e-mail: mohamed.meguid@mcgill.ca

X. Li et al. (eds.), *Proceedings of the 7th International Conference on Discrete Element Methods*, Springer Proceedings in Physics 188,
DOI 10.1007/978-981-10-1926-5_37

Layout: T1 Standard | Book ID: 417756_1_En | Book ISBN: 978-981-10-1925-8
Chapter No.: 37 | Date: 12-8-2016 Time: 2:12 pm | Page: 2/9

displacement can occur between soil and geomembrane due to different reasons, including seismic loading, waste settlement and slope movements. Fox et al. [5, 6] conducted various experiments using large-scale direct shear test machine to investigate the interface shear damage to the HDPE geomembranes when placed under coarse (i.e., gravelly) soils and over gravelly compacted clay liners (CCLs). These studies showed that interface shear displacement can cause significant more damage to geomembranes than static pressure alone.

This paper presents a coupled finite-discrete element framework that is used to investigate the response of the HDPE geomembranes subjected to static pressure and shear displacement of the interface. The specimen configuration includes HDPE geomembrane placed between gravelly soil as a drainage layer and sand as a foundation. The three-dimensional geometry of the geomembrane is properly modeled using finite elements (FE), while the soil particles are modeled using discrete elements (DE). The numerical simulation is created based on an experimental study reported by Fox et al. [6]. The main objective of this research is to examine the efficiency of the coupled FE-DE method in modelling soil-GM interaction under interface shear displacement. It should be noted that the created model is a simplification of the experimental test and the results are used to understand the behaviour of the soil-GM system.

2 Experimental Study

The experimental data was based on those reported by Fox and his group [6]. A large-scale direct shear apparatus was used to study HDPE GM-soil interaction. Figure 1a shows the specimen configuration and dimensions. Dimensions of the soil chamber are 1.064 (length) × 0.152 (width) × 0.13 m (height). The GM specimen has a thickness of 1.5 mm with blown-film texturing on both sides. The GM material properties are given in Table 1. The drainage layer consists of hard angular gravel with a particle size distribution from 25 to 38 mm. The particle size distribution of the drainage layer and also the subgrade sand layer are presented in Fig. 1b. The sand subgrade was compacted by tamping to a final thickness of 5 cm with a smooth top surface. Then the geomembrane was placed on top of the sand layer and a gravel drainage layer with 75 mm thickness was deposited on the geomembrane without compaction. A normal stress equal to 700 and 1389 kPa was applied and the specimen was sheared to a final displacement of 200 mm at a constant displacement rate of 1.0 mm/min.

Layout: T1 Standard | Book ID: 417756_1_En | Book ISBN: 978-981-10-1925-8
Chapter No.: 37 | Date: 12-8-2016 Time: 2:12 pm | Page: 3/9

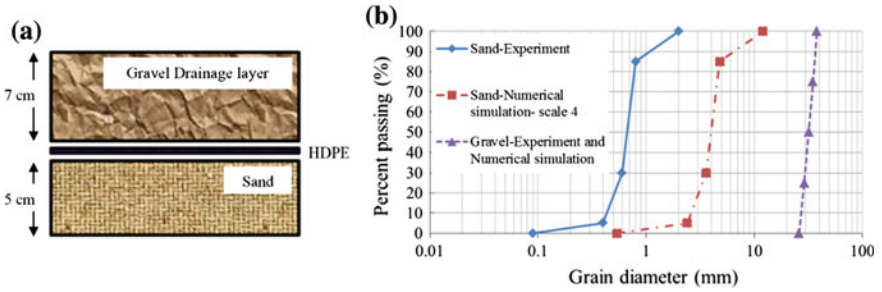

Fig. 1 **a** Specimen configuration. **b** Particle size distribution of the drainage layer and sand subgrade in the experiment and numerical simulation

Table 1 Material properties of HDPE geomembrane

Properties	Thickness	Density	Tensile strength at yield	Tensile elongation at yield
Value	15 mm	0.949 g/cc	28.4 kN/m	18 %

3 Coupled Finite-Discrete Element Framework

The coupled FE-DE framework used in this study is a continuation of the original work of Dang and Meguid [1–3]. The developed algorithm is implemented into an open source discrete element code YADE [7, 9].

Interface elements are added to the simulation to connect FE and DE domains. Triangular facets are used as interface elements generated using the finite elements coordinates. Since hexahedral elements are used for the FE domain, the contact interface between a DE particle and a FE element is divided into four triangular facets by creating a temporary center node. Figure 2 illustrates the interaction between a DE particle and interface elements created on the FE domain. The interaction between a DE particle and interface elements is similar to the particle-particle interaction. In each computational step, all particle-interface contacts are determined, and the normal penetration Δ_N and the incremental tangential displacement $\delta\Delta_T$ of each contact are calculated. Based on these values, normal and tangential forces are calculated. The contact force ($\vec{F}_{contact}$), which is determined by adding the normal and the tangential force vectors ($\vec{F}_N + \vec{F}_T$), result in the movement of DE particles and deformation of the FE domain. The FE domain deformations cause the movement of interface elements and the generation of new particle-interface interactions. A typical FE-DE computational cycle and its main steps were explained in detail by Dang and Meguid [1–3].

Layout: T1 Standard | Book ID: 417756_1_En | Book ISBN: 978-981-10-1925-8
Chapter No.: 37 | Date: 12-8-2016 | Time: 2:12 pm | Page: 4/9

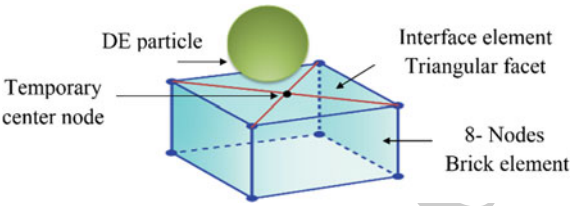

Fig. 2 Coupling FE and DE using interface elements

4 Model Generation

The numerical model is developed such that it follows the geometry and the test procedure used in the actual experiment. The geomembrane, including 8 transverse elements and 67 longitudinal elements, is modeled using 8-noded brick elements with 8 integration points (Fig. 3). The length of the geomembrane is kept 20 cm longer than the soil chamber from the rear side to ensure a constant friction between the soil and the geomembrane during the test. A linear elastic material model is used for the geomembrane and its properties are obtained from Table 1. The full geometry of the geomembrane, consisting of 536 finite elements and 4288 interface elements, is illustrated in Fig. 3.

The drainage layer of gravelly soil in the experiment is modeled using spherical particles. The particle size distribution is the same as that used in the experiments as presented in Fig. 1b. To generate this layer, a set of non-contacting particles are first generated. Then, all particles are allowed to move under the gravity without compaction. A total of 423 gravel particles are generated with the final thickness similar to that in the experiment: 75 mm. The sand used as a subgrade in the experimental test is modeled using spherical particles. Since it is numerically impossible to simulate millions of particles using the actual size distribution, up-scaling is required to keep the duration of the simulation within a reasonable time limit. Among the several packing algorithms developed to generate the discrete element specimen, the radius expansion method is used in this study to generate the pack with specific porosity. A cloud of non-contacting spherical particles is generated, and radii of particles are increased to reach the target porosity of 0.4. Then, the sand specimen is allowed to move under the gravity until the pack reaches the static equilibrium condition. Using a scale factor of 4, a total of over 50,000 particles are generated to replicate the sand subgrade. A partial 3D view of the completely generated sample is shown in Fig. 4.

To determine the input parameters of discrete particles, calibration is needed. Since results from laboratory tests (Triaxial and direct shear test) for the drainage layer and the subgrade soil are not available, a parametric study is conducted instead to determine the effect of the input parameters on the shear stresses. The microscopic friction angle of interface elements ($\emptyset_{micro}$), Young's modulus of gravel particles (E_i), the ratio between tangential and normal stiffness of particles (K_T/K_N), and the rolling resistance coefficient β_r are selected for the parametric study. Table 2 shows the input parameters chosen for the simulation.

Layout: T1 Standard | Book ID: 417756_1_En | Book ISBN: 978-981-10-1925-8
Chapter No.: 37 | Date: 12-8-2016 | Time: 2:12 pm | Page: 5/9

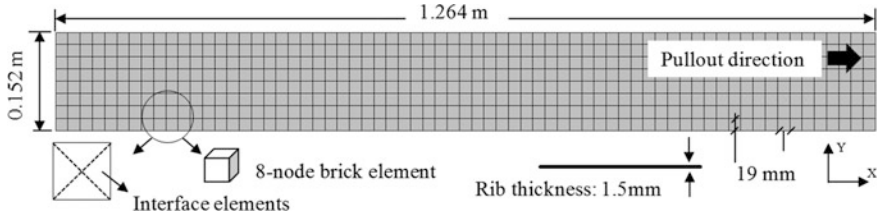

Fig. 3 Geometry of the geomembrane

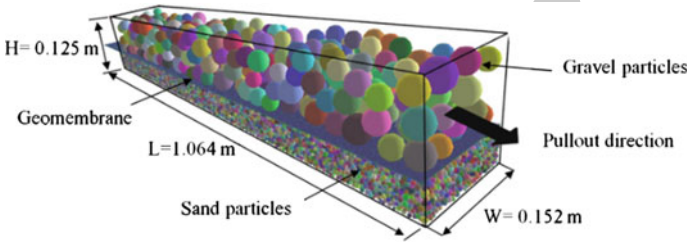

Fig. 4 Initial FE-DE specimen

Table 2 Input parameters of the simulation

Discrete particles	Value	Finite elements (GM)	Value
Density of gravel particles (kg/m^3)	2750	Young's modulus E (MPa)	800
Density of sand particles (kg/m^3)	2600	Poisson's ratio ν	0.3
Gravel particle modulus E (MPa)	200		
Sand particle modulus E (MPa)	60		
Ratio K_T/K_N	0.3	Interface elements	Value
Micro friction angle of gravel particles	40°	Material modulus E (MPa)	100
Micro friction angle of sand particles	30°	Ratio K_T/K_N	0.3
η_r	1.0	Micro friction angle ($\emptyset_{micro}$)	30°
Rolling resistance coefficient (β_r)	0.3		
Damping coefficient	0.2		

After creating the final particle assembly in the box and assigning the input parameters, normal stresses equal to 700 and 1389 kPa are applied on the drainage layer, and the geomembrane is allowed to deform freely. Then, pullout force is applied to the first row of FE nodes of the geomembrane using a displacement control approach with a rate similar to that of the experiment. At each displacement step (0.005 m), movements of the first row of FE nodes are stopped until convergence conditions are satisfied in both DE and FE domains. Additional frontal displacements are then applied in subsequent steps, and the procedure continues until the frontal displacement reaches 50 mm.

Layout: T1 Standard | Book ID: 417756_1_En | Book ISBN: 978-981-10-1925-8
Chapter No.: 37 | Date: 12-8-2016 Time: 2:12 pm | Page: 6/9

5 Result and Discussion

5.1 Shear Stress-Displacement Relationship

The relationship between the geomembrane shear stress and its displacement is shown in Fig. 5. It can be seen that the FE-DE results for both normal stresses (700 and 1389 kPa) are similar to those of the experimental data. The differences in the maximum shear stress and its location can be attribute to the uncertainty on input parameters for the drainage layer and the subgrade soil. Also, the sandy subgrade porosity and its relative density are needed in the pack generation. As mentioned before, the main objective of this study is to examine the efficiency of the coupled FE-DE framework in modeling soil-GM interaction in shear mode. Hence, considering the simplifications made in the DE simulation, the calculated results are acceptable and useful to understand the behavior of soil-GM interaction.

Figure 6 shows the effect of different input parameters on the shear stress magnitude. Increasing the micro friction angle of the interface elements will increase the maximum shear stress of the geomembrane (Fig. 6a). Similarly, increasing the gravel particles modulus (E) increases the shear stress value (Fig. 6b). Also, changing in the ratio of the tangential stiffness to the normal stiffness of particles (K_T/K_N) has the same effect on maximum shear stress (Fig. 6c). On the other hand, increasing the rolling resistance coefficient (β_r) decreases the maximum shear stress (Fig. 6d). It can be seen that changing the input parameters has an effect on the shear stress, and the maximum shear stress is more sensitive to the ratio of the tangential stiffness to the normal stiffness of particles (K_T/K_N) among the different parameters.

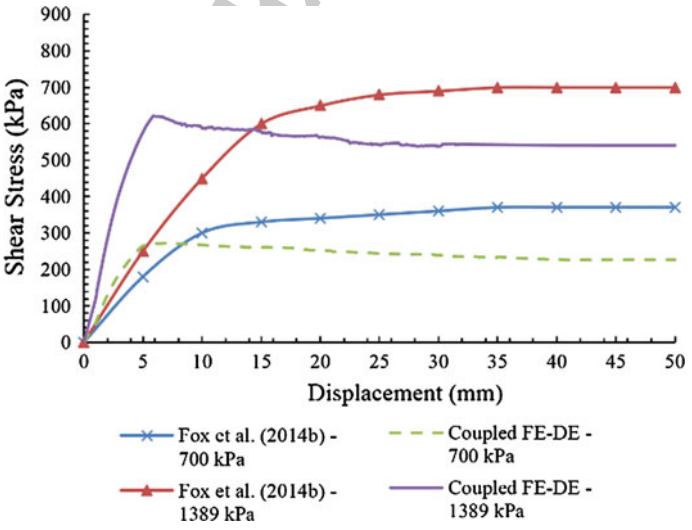

Fig. 5 Shear stress-displacement relationship

Layout: T1 Standard | Book ID: 417756_1_En | Book ISBN: 978-981-10-1925-8
Chapter No.: 37 | Date: 12-8-2016 Time: 2:12 pm | Page: 7/9

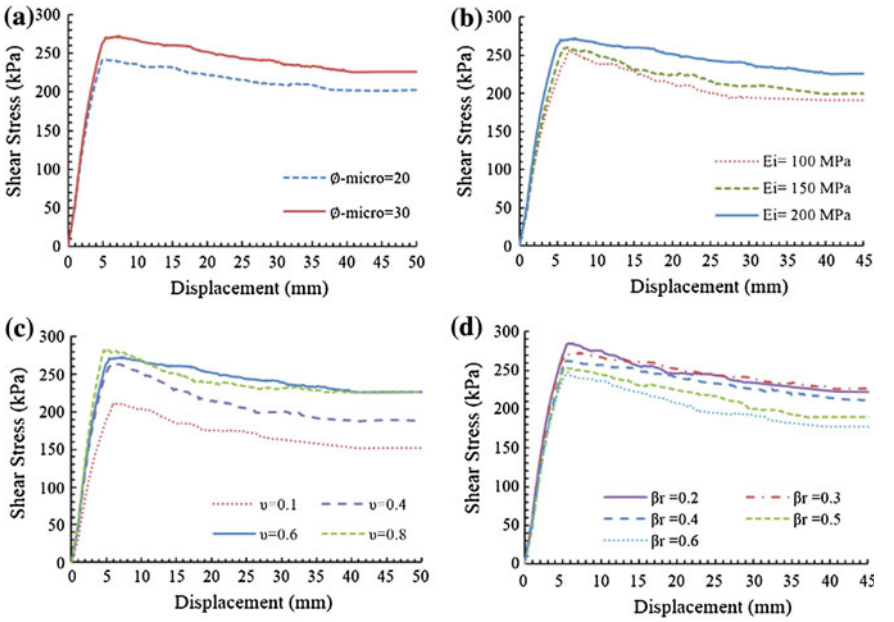

Fig. 6 Dependency of shear stress-displacement relationship to different parameters **a** interface friction angle, **b** gravel particle modulus, **c** stiffness ratio, **d** rolling resistance coefficient

The main outcome of this parametric study is that calibration is a fundamental step in the DE simulation, and micro parameters have significant effects on the final results.

5.2 Response of the Geomembrane

The geomembrane vertical deformation (υ_z) for frontal displacements of 0 and 20 cm under the vertical stresses of 700 and 1389 kPa are shown in Figs. 7 and 8. Before applying the pullout force, the largest deformation of the geomembrane is found to be around 4 mm in the moderate normal stress condition (700 kPa) and around 6 mm under the high normal stress level (1389 kPa). After the shearing stage, vertical deformation increases in both conditions, and the maximum deformation reaches 8 mm in moderate normal stress condition and exceeds 10 mm under the high normal stress level. Hence, prior to the shearing stage, minor indentations occurred in the geomembrane from the stress concentration of the overlaying gravel layer. But, after the shearing displacement to 20 cm, the level of indentation as a damage, and the number of points with significant deformation are increased dramatically. The level of damage due to the indentation is larger in the high normal stress condition than the moderate (Figs. 7b vs. 8b). These results are similar to the observations reported by Fox et al. [6]. For instance, Fig. 9 shows a

Layout: T1 Standard | Book ID: 417756_1_En | Book ISBN: 978-981-10-1925-8
Chapter No.: 37 | Date: 12-8-2016 Time: 2:12 pm | Page: 8/9

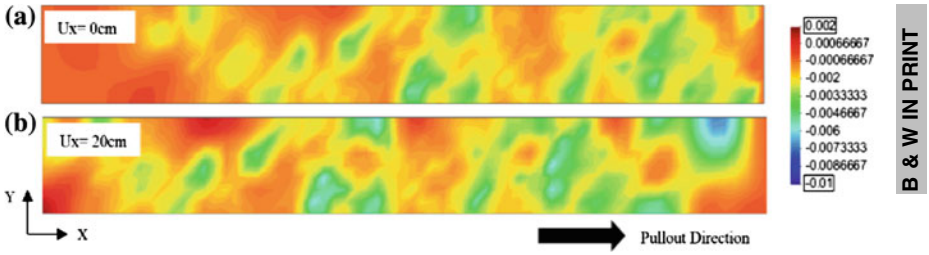

Fig. 7 Vertical displacement (m) of the geomembrane **a** before and **b** after the sharing under moderate normal stress level (700 kPa)

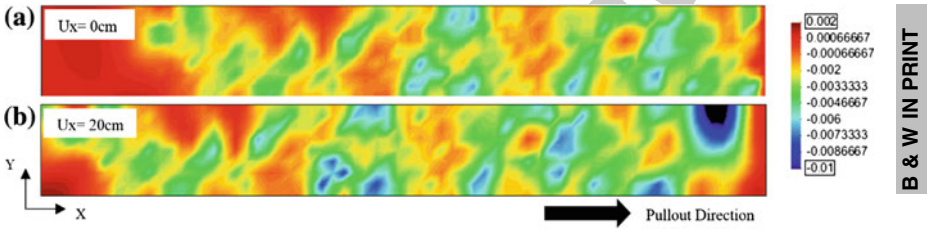

Fig. 8 Vertical displacement (m) of the geomembrane **a** before and **b** after the sharing under moderate normal stress level (1389 kPa)

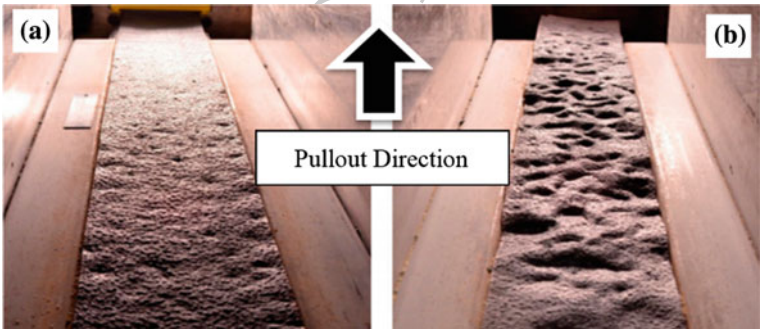

Fig. 9 GM after **a** static pressure (1389 kPa) and **b** shearing stage—Fox et al. [6]

photograph of a geomembrane under static pressure equal to 1389 kPa (Fig. 9a) and after the shearing stage (Fig. 9b). It can be seen that major indentation occurred on the geomembrane after applying the shear displacement.

Layout: T1 Standard | Book ID: 417756_1_En | Book ISBN: 978-981-10-1925-8
Chapter No.: 37 | Date: 12-8-2016 Time: 2:12 pm | Page: 9/9

References

1. Dang, H.K., Meguid, M.A.: Algorithm to generate a discrete element specimen with predefined properties. Int. J. Geomech. **10**(2), 85–91 (2010)
2. Dang, H.K., Meguid, M.A.: Evaluating the performance of an explicit dynamic relaxation technique in analyzing nonlinear geotechnical engineering problems. Comput. Geotech. **37**(1), 125–131 (2010)
3. Dang, H.K., Meguid, M.A.: An efficient finite-discrete element method for quasi-static nonlinear soil-structure interaction problems. Int. J. Numer. Anal. Meth. Geomech. **37**(2), 130–149 (2013)
4. Fox, P.J., Nye, C.J., Morrison, T.C., Hunter, J.G., Olsta, J.T.: Large dynamic direct shear machine for geosynthetic clay liners. J. ASTM Geotech. Test. **29**(5), 392–400 (2006)
5. Fox, P.J., Thielmann, S.S., Stern, A.N., Athanassopoulos, C.: Interface shear damage to a HDPE geomembrane. I: gravelly compacted clay liner. J. Geotech. Geoenviron. Eng. (2014). doi:10.1061/(ASCE)GT.1943-5606.0001132,04014039
6. Fox, P.J., Thielmann, S.S.: Interface shear damage to a HDPE geomembrane. II: gravel drainage layer. J. Geotech. Geoenviron. Eng. (2014). doi:10.1061/(ASCE)GT.1943-5606.0001120,04014040
7. Kozicki, J., Donze, V.F.: YADE-OPEN DEM: an open-source software using a discrete element method to simulate granular material. Eng. Comput. **26**(7), 786–805 (2009)
8. Rowe, R.K., Quigley, R.M., Brachman, R.W.I., Booker, J.R.: Barrier systems for waste disposal facilities, 2nd edn. Spon, London (2004)
9. Smilauer, V., Catalano, E., Chareyre, B., Dorofeenko, S., Duriez, J., Gladky, A., Kozicki, J., Modenese, C., Scholtès, L., Sibille, L., Stránský, J., Thoeni, K.: Yade Documentation. The Yade Project 2010 (2010). http://yade-dem.org/doc

AQ2